Review Paper

Therapeutic Metallic Ions in Bone Tissue Engineering: A Systematic Review of The Literature

Hannaneh Safiaghdam[a], Hanieh Nokhbatolfoghahaei[b,c] and Arash Khojasteh[b,c*]

[a]Student Research Committee, Dental school, Shahid Beheshti university of medical sciences, Tehran, Iran. [b]Department of Tissue Engineering and Applied Cell Sciences, School of Advanced Technologies in Medicine, Shahid Beheshti University of Medical Sciences, Tehran, Iran. [c]Dental Research Center, Research Institute of Dental Sciences, Shahid Beheshti University of Medical Sciences, Tehran, Iran.

Abstract

An important field of bone tissue engineering (BTE) concerns the design and fabrication of smart scaffolds capable of inducing cellular interactions and differentiation of osteo-progenitor cells. One of these additives that has gained growing attention is metallic ions as therapeutic agents (MITAs). The specific biological advantage that these ions bring to scaffolds as well as other potential mechanical, and antimicrobial enhancements may vary depending on the ion entity, fabrication method, and biomaterials used. Therefore, this article provides an overview on current status of *In-vivo* application of MITAs in BTE and the remaining challenges in the field. Electronic databases, including PubMed, Scopus, Science direct and Cochrane library were searched for studies on MITAs treatments for BTE. We searched for articles in English from January-2000 to October-2019. Abstracts, letters, conference papers and reviews, *In-vitro* studies, studies on alloys and studies investigating effects other than enhancement of new bone formation (NBF) were excluded. A detailed summary of relevant metallic ions with specific scaffold material and design, cell type, animal model and defect type, the implantation period, measured parameters and obtained qualitative and quantitative results is presented. No ideal material or fabrication method suited to deliver MITAs can yet be agreed upon, but an investigation into various systems and their drawbacks or potential advantages can lead the future research. A tendency to enhance NBF with MITAs can be observed in the studies. However, this needs to be validated with further studies comparing various ions with each other in the same animal model using critical-sized defects.

Keywords: Bone tissue engineering; Metallic ions; Scaffolds; Therapeutic ions; Dug delivery

Introduction

Successful induction of bone tissue regeneration is a complicated process requiring harmonic interplay of cells, cell supporting scaffolds and bioactive materials (1). An important field of bone tissue engineering (BTE) concerns the design and fabrication of smart scaffolds capable of inducing cellular interactions and differentiation of osteo-progenitor cells. This can be achieved by loading the engineered scaffold with various therapeutic agents that give the scaffold a dual function: as a bed for new tissue growth and as a carrier for controlled in-situ drug delivery (2). One of these additives that has gained growing

* Corresponding author:
   E-mail: arashkhojasteh@gmail.com

attention is metallic ions as therapeutic agents (MITAs). As it has been shown in the recent literature that some ions are able to guide the differentiation of stem cells into a desired path, there is great hope in employing them in regenerative medicine (3-5). MITAs have essential roles in body as cofactors of various enzymes, in cellular metabolism, signaling pathways, ionic channels and other biologic procedures (6). Metallic ions enhance osteogenic differentiation of mesenchymal stem cells & regulate osteoclast-mediated bone resorption. Pathways known to be involved in osteogenic differentiation such as Wnt signaling has been reported to be influenced by stimulation with trace ions like lithium, magnesium, strontium, or zinc (7). Other related osteogenic markers such as Runt-related transcription factor 2 (Runx2), osteonectin, osteopontin, and collagen type one are also enhanced with addition of metallic ions (8-12). MITAs also have a role in promoting differentiation, migration and capillary formation of endothelial cells as well as inducing secretion of pro-angiogenic factors such as vascular endothelial growth factor (VEGF) (13-15). Inorganic ions are also bacteriostatic which give the scaffold impunity against bacterial adhesion & infection which disturb tissue integration (16, 17). Moreover, MITAs have relatively lower risk of cancer compared with recombinant proteins or genetic modifications (18). The bioactivity of a bone scaffold depends on the interaction of its constituent molecules with stem cells and pre-osteoblasts at the interface (19). Along with the growth factor proteins such as bone morphogenetic protein (BMP) family or other peptides and small molecules, research has been focused on metallic ions (20-22). Their prominent advantages against growth factors and other organic drugs are the lower expense, relative stability during fabrication procedure and higher function in lower concentrations (21, 23). Local delivery of these metal ions compared to taking them via oral routes has the advantage of better control over dose and distribution of the drug (24). Moreover, the ionic state of a few metallic ions is unstable and may cause toxic effects in case of direct ingestion. In case of systemic distribution, non-specific adverse effects in neurologic,

cardiologic, hematologic or endocrine systems may be observed (25, 26). It should be noted that designing a scaffold that regulates the specific amount of ion released in a particular period is necessary to prevent local toxic effects and ion's side effect on the metabolism of adjacent cells (27). Modulating release kinetics of ions from scaffold in a controlled manner, reduces the accumulation of ion and dose-dependent toxicity and results in induction of favorable cell behavior (3). Different methods such as Ion exchange, solvent casting, salt leaching, electrospinning, three dimensional (3D) printing, freeze-drying, and laser sintering have been applied in fabrication of bone scaffolds incorporating MITAs (28-33). These inorganic ions can be incorporated into various materials such as bioactive glasses, glass ceramics, calcium phosphates, hydroxyapatite (HA), alpha and beta-tricalcium phosphates, biodegradable polymers and composite scaffolds. This addition alters degradation behavior, mechanical characteristics and biological function of scaffolds (34). In this systematic review, we aimed to analyze *In-vivo* studies on MITAs less commonly applied in BTE and present an overview upon their efficacy in enhancing bone regeneration.

Experimental

This study has been designed and conducted according to the preferred reporting items for systematic reviews and meta-analyses (PRISMA) guidelines (35). Electronic databases, including PubMed, Scopus, Science direct and Cochrane library were searched for studies on MITAs treatments for BTE. The following keywords were used: bone tissue engineering/bone substitute/scaffold [title/abstract] AND ion/mineral/names of organic ions each searched separately [title/abstract]. We searched for articles in English from January 2000 to October 2019 and checked the reference list of related reviews and the following journals for additional relevant studies: (1) Biotechnology and Bioengineering; (2) Journal of Biomedical Materials Research; (3) Journal of Tissue Engineering; (4) and Acta Biomateralia. A total of 1405 articles were collected. Eligibility checking and data extraction were

performed independently by two reviewers. Any disagreements were resolved by discussion. Inclusion and exclusion criteria of the study were applied through the initial screening of titles and abstracts. Total of 284 duplicate results were excluded. Abstracts, letters, conference papers, and reviews were excluded (n=3). Abstracts and titles were screened and 1055 articles were excluded as they were *In-vitro*. Full-texts for the remainder were obtained (n = 63). Studies on alloys & mixtures of ions (n=19) were excluded because the osteoinductive activity could not be completely attributed to the one specific component. Also studies investigating ion effects other than enhancement of new bone formation (NBF) (n = 10) were excluded. One study was excluded because of the unacceptable *In-vivo* model. Figure 1 shows a diagram of study selection process.

The included studies were screened for the scaffold and fabrication method, cell type used, the animal model and size & location of the defect, the implantation period, study groups, measured parameters and obtained qualitative and quantitative results. A meta-analysis could not be conducted due to the heterogeneity of the data.

Results

A total of 33 articles met our inclusion and exclusion criteria and were reviewed. The data is summarized in Table 1. Studies were classified according to the metallic ion added to the scaffolds. Strontium was the most studied ion, with 13 *In-vivo* studies (12, 36-47), followed by magnesium with 6 (9, 30, 48-51) and zinc with 5 articles (22, 52-55). Two articles were found on silicon (10, 56), lithium (8, 57) and iron (58, 59) each, and copper (60), silver (61), and cobalt (62, each had only one studies.

These metallic ions were incorporated into various scaffolds: A total of 11 articles used polymers such as poly-caprolactone (PCL) (n = 5) (10, 37, 38, 48, 51), poly lactic-co-glycolic acid (PLGA) (n=2) (9, 30), Poly-L-lactic acid (PLLA) (n = 2) (39, 61), chitosan (60), and combination of collagen and alginate (62). Among the 13 studies which used ceramics, six used hydroxyapatite (HA) (8, 46, 49, 53,

56, 58), four used calcium polyphosphates (CPP) (43-45, 57), three used tricalcium phosphate (TCP) (22, 54, 55). One study used magnesium phosphate 2D nano-sheets (50). Another ten studies evaluated the efficacy of ions in composite scaffolds. HA was used in combination with collagen in 3 studies (47, 52, 53), with poly(γ-benzyl-l-glutamate) (PBLG) in 2 studies (40, 63), with PCL in 2 other studies (36, 61), and with PLLA in one study (41). Collagen polymer was combined with amorphous calcium phosphate porous microspheres in a study on strontium ion (52).

Only six studies implanted the designed scaffolds with stem cells to enhance bone formation. These included rabbit adipose derived stem cells (ADSCs) (40), rabbit bone marrow derived stem cells (BMSCs) (45), mice ADSCs (42), human telomerase immortalized BMSCs (37), hypoxia preconditioned BMSCs (8), and finally MC3T3e1 (mouse pre-osteoblast) cell lines (10).

Most frequently used animal model was rat (n=17) followed by rabbit (n=12). Two studies used mice while one study reported beagle dog (30) and another reported goat (64) as its animal model.

The most commonly used defect model was a critical sized calvarial defect. Two studies investigated NBF in 8 mm defects (9, 61) while seven used 5 mm defects (12, 36, 39, 46, 56, 60, 62). A 15 mm defect was used in a goat model calvarium (49), as well as a 10 mm rabbit calvarial defect (43) and a 2mm mouse cranial defect (38). One infected cranial defect was used to evaluate the antimicrobial effect of silver along with osteoinductivity (61). Eleven femoral (22, 40-42, 44, 51-53, 55, 58, 59), five tibial (8, 47, 50, 57, 65) and one radial defects (45) were also studied in varying dimensions considered to be critical. Subcutaneous implantation was applied in 3 studies (10, 37, 48) and one study reported a split mouth socket preservation in a dog model (30).

Average implantation period was 11.27 weeks which varied between one study evaluating NBF after 2 weeks (50) and another long-term study waiting for a maximum of 60 weeks (55). However, most of the studies (n=11) had a 12-week implantation period, followed by 10 studies having an 8-week period.
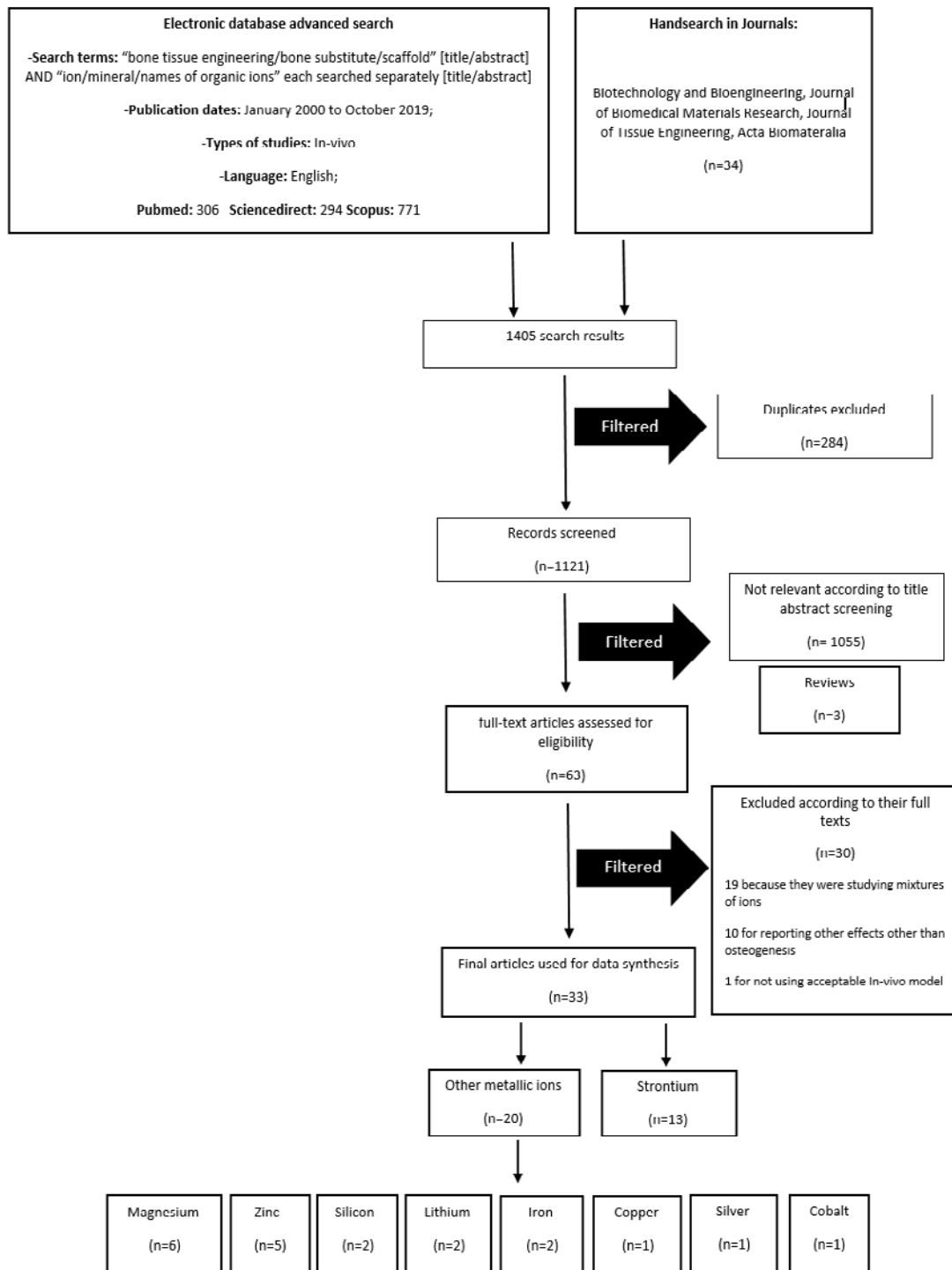
Figure 1. PRISMA Flowchart.

Table 1. Metallic ions other than strontium used in bone tissue engineering by order of frequency and published year.

Author (year)	Ion	scaffold	Ion addition method	Cell type	Animal model	Defect size & location	Implantation period	Groups	Parameters	Observed effect	Ref
Wei (2018)	Ag	PLLA + nano silver + polydopamine + PEG	W1/O/W2 double emulsion method	-	SD rat	Infected 8mm critical-sized calvarial defect	8 W	A. PEG10% +polydopamine + PLLA B. PEG% + polydopamine + PLLA + Ag C. Empty	H&E / *In-vitro* incubation of granulation tissues to observe the bacterial growth	The Ag group showed much reduced infection in comparison to other groups / NBF was higher in Ag	(61)
Perez (2015)	Co	Collagen + BMP2 + alginate + Co	Crosslinking	-	male SD rat	5 mm critical sized calvarial defects	6 W	A. no Co/BMP2, B. Co only C. BMP2 only D. Co/BMP2 both	μ-CT / H&E	Most calcified tissue type in Co with BMP2 / Bone volume: Co only (11.30 ± 2.00 %) < bare (14.51 ± 2.45 %) < BMP2 only (29.94 ± 2.53 %) < Co with BMP2 (35.10 ± 2.81 %)	(62)
D'Mello (2014)	Cu	Cu + chitosan	Freeze-drying	-	Male Fisher 344 rat	5 mm critical sized calvarial defect	4 W	A. empty B. chitosan C. Chitosan + Cu	μ-CT / H&E	NBF increased with copper BV/TV: copper-chitosan= 11x empty defects and 2x chitosan scaffolds	(60)
Russo (2017)	Fe	HA + Magnetite (90-10%)	Homogeneous mixed slurry	-	Male rabbit	6x8 mm Critical size femoral defect	4,12 W	A. HA B. HA + Magnetite	Toluidine Blue / Acid Fuchsin / Fast Green / TRAPP	NBF% 4th week: A: 35 ± 4 B: 19 ± 4 / NBF 12th week: A: 29 ± 6 B: 15 ± 5	(58)
De Santis 2015)	Fe	PCL + HA + Fe (80-20%)	Mixing and using ultrasonic bath	-	Male rabbits (Oryctolagus cuniculus)	6x8 mm Critical size femoral defect	4W	A. PCL B. PCL/FeHA	Toluidine Blue / Acid Fuchsin / Fast Green	A similar to B	(59)
Ma (2018)	Li	CPP + Li	chemical precipitation	-	adult male Japanese white rabbits	Bilateral 3x5 mm tibial defect	4, 8 W	A. 0.1%LiCPP B. 1.0%LiCPP C. 2.0%LiCPP D. 3.0%LiCPP E.CPP	H&E	NBF: C>B>E	(57)
Li (2018)	Li	HA + Li	chemical precipitation	BMSCs	male Japanese white rabbits	5 mm diameter tibial defect	6, 12 W	A. 1.5% Li- HA + hypoxic BMSCs B. 1.5%Li-HA + normal BMSCs C. 1.5%Li-HA D. HA	μ-CT / H&E / MT / IHC / qRT-PCR / Western blot	BV/TV%: A>B>C>D / NBF: A>B>C>D	(8)
Yuan (2018)	Mg	PLGA + MgO + MgCO3	W1/O/W2 double emulsion method	-	female SD rat	8 mm critical size calvarial defect	4,8,16 W	A. PLGA B. PLGA + MgO + MgCO3 in 1:1 C. Empty	μ-CT / H&E / MT / IHC	BV/TV B: 32.9 ± 5.6 % A: 8.1 ± 2.5 % / BMD B: 325.7 ± 20.2 A: 124 ± 35.8	(9)
Suryavanshi (2017)	Mg	PCL + MgO 10%	precipitation-calcination method	-	SD rat	subcutaneous implantation	2, 4, 8 W	A. PCL B.PCL + Mgo	H&E	Higher cell infiltration and NBF & Higher OCN and OPN In B No NBF / Proved biocompatibility	(48)

Continued Table 1. Metallic ions other than strontium used in bone tissue engineering by order of frequency and published year.

Author (year)	Ion	scaffold	Ion addition method	Cell type	Animal model	Defect size & location	Implantation period	Groups	Parameters	Observed effect	Ref
Deng (2017)	Mg	HA + Mg + rhBMP2	chemical precipitation	-	Goat	Bi-parietal 15 mm calvarial defect	4,8,12 W	A. HA + Mg + rhBMP-2 / B. HA + Mg / C. HA	H&E / MT / CT / qRT-PCR	Gray value & VEGF and ColI & Mean osteogenic area: A>B>C	(49)
Laurenti (2016)	Mg	2D Magnesium Phosphate Nanosheets	percipitation method	-	Rat	Tibia defect	3 days 1,2 W	A. Nano MgP / B. empty	µ-CT / H&E / qRT-PCR	NBF: MgP > empty / Defect fully filled at 14days / Runx2 and ColI expressed more at day3 in MgP	(50)
Brown (2015)	Mg	PLGA + Mg	Solvent casting, salt leaching	-	Beagle dog	Split mouth socket preservation	8,16 W	A. PLGA + 10 mg Mg / B. Empty	µ-CT / MT / Von kossa staining / Chloroacetate esterase staining	Upregulation of osteoclasts / Defect height 8th week A:1.9 B:2.2mm / Defect height 16th week A:0.9 B:1.6 / BV/TV 8th week: A:29% B:21% / BV/TV 16th week: A:35% B:31%	(30)
Wong (2014)	Mg	PCL + Mg	Salt leaching	-	Female SD rat	Bilateral 2x6 mm femoral defect	12 W	A. PCL / B. Silane coupled Mg-PCL	Giemsa Staining	No sign of chronic inflammation NBF & osteoblast B>A	(51)
Wang (2018)	Si	PCL + nano Si (0%, 1%, 5%, and 10% w/w)	Mixing and using Itrasonic bath	MC3T3 e1 cells	female & male SD rats	Subcutaneous implantation	1,4 W	A. 1.0% nano-Si PCL / B. 10% nano-Si PCL / C. PCL	H&E / MT / IHC	Higher calcification & Higher OCN In B	(10)
Cui (2016)	Si	Si-HA + BMP-2-related peptide (P28)	Freeze-drying	-	male SD rat	5 mm critical size calvarial defect	6, 12 W	A. empty / B. Si/HA / C. Si/HA + P28 / D.Si/HA + rhBMP2	µ-CT / H&E	NBF 6th week A: 9.44 ± 2.20% B: 16.22 ± 2.31% C: 49.99 ± 5.51% D: 51.15 ± 3.46% / NBF 12th week: A: 21.94 ± 1.86% B: 36.39 ± 3.57% C: 84.18 ± 6.03% D: 86.63 ± 3.82%	(56)
Samanta (2019)	Zn	βTCP +5% Zn or Mg or Ti	aqueous solution combustion technique	-	rabbits	5 ×2.5 ×3 mm Femoral defect	4,8 W	A. Empty / B. βTCP / C. βTCP + Zn / D. βTCP + Mg / E. βTCP + Ti	µ-CT / X-ray radiography / H&E / SEM / IHC	BV/TV: C=D=B>A / NBF 1st month: A: 16.39 ± 1.9 B: 27.48 ± 1.9 C: 35.64 ± 2.0 D: 41.35 ± 2.0 E: 50.31 ± 1.9 / NBF 2nd month: A: 30.53 ± 2.0 B: 34.24 ± 2.0 C: 48.40 ± 2.0 D: 50.55 ± 2.0 E: 65.06 ± 3.0	(22)

Continued Table 1. Metallic ions other than strontium used in bone tissue engineering by order of frequency and published year.

Author (year)	Ion	scaffold	Ion addition method	Cell type	Defect size & location	Implantation period	Groups	Parameters	Observed effect	Ref
Yu (2017)	Zn	HA/COL + Zn	lyophilization fabrication	-	3.5x4 mm critical size femoral condyle defect	8 W	A. HA/Col B. HA/COL + Zn Zn/(Zn + Ca) molar ratios of 0 C. HA/COL + Zn Zn/(Zn + Ca) molar ratios of 0.05	μ-CT H&E	BV/TV A:22.87%±4.46 B:40.18%±4.41% C: 76%±4.46% NBF A: 13.16%±3.92% B: 32.55%±5.66% C: 42.27%±5.74%	(52)
Begam (2017)	Zn	HA + Zn OR HA/COL + Zn + BMP2	Wet chemical method	-	4x5 mm Femoral defect	12W	A. Zn + HA B. Zn + HA + BMP2 C. Zn + HA /COL + BMP2	H&E SEM IHC H&E of liver and kidney (toxicology)	NBF: B > C Kidney and liver normal	(53)
Chou (2013)	Zn	Zn-TCP	hydrothermal conversion	-	2x3 mm tibial defect	8 W	A. Zn-TCP B. βTCP C. Empty	μ-CT H&E CT	faster rise in bone mineral density in A compared to B or C but BMD at 8th week: A=B restoration of the trabecular bone in the A was more mature and dense compared with B both A & B were able to stimulate regeneration of new bone closing the defect, but were also regenerating cancellous bone	(65)
Kawamura (2003)	Zn	TCP+ Zn + HA	Sol-Gel method	-	Transcortical Femoral defect	2-60 W	A. ZnTCP, TCP, and HAP powders B. TCP/HAP composite ceramic	IHC	The Change in cortical bone apposition rate (C-BAR) 24th week A: 85.3 ± 6.0% B: 70.8 ± 6.9% C-BAR 60th week A: 74.5 ± 17.5% B:52.6 ± 10.3% Change in intramedullary bone apposition rate (IM-BAR) 6th week A: 61.4 ± 26.7% B: 42.6 ± 18.5% Medullary cavity area (MCA) A: 15.7 ± 3.9 B: 12.2 ± 3.7	(55)

ACP: amorphous calcium phosphate; ADSCs: Adipose derived stem cells; Ag: Silver; BIC: Bone to implant contact; BMD: Bone mineralization density; BMP2: Bone morphogenetic protein 2; Br: Bromium; BV/TV: bone mineral volume/total volume ratio; CaP: Calcium phosphate; Co: Cobalt; ColI: Collagen Type I; CPP: Calciumpolyphosphate; Cu: Copper; DEXA: Dual-energy X-ray absorptiometry; F:Fluoride; Fe: Iron; HA: hydroxyapatite; H&E: hematoxylin and eosin staining; HU: Hansfield Units; HPMC: (Hydroxypropyl)methyl cellulose; IHC: Immunohistochemistry; Li: lithium; Mg: Magnesium; MT: Masson's trichrome staining; NBF: New Bone Formation; OCN: osteonectin; OPN: Osteopontin; PCL: polycaprolactone; PEG: poly(ethyl glycol); PIB: p(N-isopropylacrylamide-co-butyl methylacrylate); PLGA: poly-(lactide-co-glycolide); PLLA: poly(l-lactide); qRt-PCR: Quantitative Real time polymerase chain reaction; rhBMP2: Recombinant human bone morphogenic protein 2; SD: Sprague Dawley rats; Si: Silicon; SPES: sulfonated poly(ether sulfone); TRAPP: Tartrate-resistant acid phosphatase-positive; VEGF: vascular endothelial growth factor; W: weeks; W1/O/W2: water-in-oil-in water; WH:whitlockite; Zn: Zinc.

Table 2. Strontium in bone tissue engineering

| Author (year)	Scaffold	Fabrication method	Cell type	Animal model	Defect size & location	Implantation period	Groups	Parameters	Observed effect	Ref
Liu (2019)	PCL + HA + Sr	3D printing	-	SD rats	5 mm critical Size calvarial defect	12 W	A. PCL B. PCL + HA C. PCL + HA + Sr	μ-CT H&E MT	NBF: C>B>A	(36)
Prabha (2019)	PCL + SRA	Solution blending method	human telomerase immortalized bone marrow derived keletal stem cell line (hMSC-TERT)	NOD.B17-Prkdcscid/J mice	Subcutaneous implantation	8 W	A.PCL + cell B. PCL + SRA + cell C. PCL D.PCL + SRA	H&E HVM Sirius red	matrix was rich in Type I collagen areas of vascularized ectopic bone matrix formation was seen	(37)
Lino (2018)	PCL + PDIPF + 1% or 5% Sr	Solvent casting	-	WKAH/Hok Wistar rats	2 mm calvarial defect	4W	A.PCL/PDIPF B. PCL/PDIPF + 1%Sr C. empty	H&E qRT-PCR	NBF: B= A + 52% Runx2: C>B>A	(38)
Han (2019)	PLLA + Sr	electrospinning	-	SD rat	5 mm critical size calvarial defect	8W	A. PLLA B. PLLLA C. PLLLA + 5 Sr D. PLLLA + 10 Sr E. PLLLA + 15 Sr	μ-CT H&E MT Gieson IHC	NBF: E>D>C>B>A CA A:0.297 ± 0.085% B:0.657 ± 0.17%) C: 1.26 ± 0.079% D:1.37 ± 0.085% E: 1.657 ± 0.13%, AR: A:0.397±0.148%, B:0.793±0.194%, C:1.133±0.1%, D:1.647±0.107% E:1.97±0.123% 0.05 TE: A:0.277±0.1% B:0.337±0.08% C:0.737±0.102% D:1.337±0.111% E:1.427±0.135%	(39)
Yan	HA + PBLG +Sr	coprecipitation + aminated surface modification	Rabbit ADSCs	New Zealand rabbit	Critical full-thickness segmental Femoral defect	12, 24 W	A. HA + PBLG +Sr B. HA + PBLG +Sr+ ADSCs	μ-CT H&E MT	B>A	(40)
Ge (2018)	PLLA + HA + Sr	lyophilization	-	JW rabbits	3.5 mm femur defect	5W	A. PLLA B. PLLA + HA C. PLLA + HA + Sr	μ-CT H&E MT	NBF: C>B>A=0	(41)
Yu (2017)	APMs + COL + Sr	Microwave-Hydrothermal Method	-	SD rat	5mm critical size calvarial defects	8 W	A. Col B. APMs/col C.SrAPMs/col	μ-CT H&E IHC	BMD: A: 55.88 ± 14.89 B: 213.12 ± 52.05 C: 334.78 ± 41.08 BV/TV: A: 3.36 ± 0.76% B: 20.64 ± 7.33% C: 48.30 ± 11.75% NBF: C>B>A OCN & OPN: C>B	(12)

Continued Table 2. Strontium in bone tissue engineering

Author (year)	Scaffold	Fabrication method	Cell type	Animal model	Defect size & location	Implantation period	Groups	Parameters	Observed effect	Ref
Gao (2017)	HA + PBLG + Sr	covalent surface functionalization	Mouse ADSCs	C57BL6/J mice	2mm critical size in middle femur	8W	A. HA + PBLG + Sr B. HA + PBLG + Sr + ADSCs	x-ray radiography μ-CT	NBF: B>A BV/TV: B= normal bone > A	(42)
Wang (2016)	SCPP	gravity sintering	-	New Zealand white rabbits	10mm critical size calvarial defects	4,8,12 W	A. Sr.SCPP B. DOPA/Sr.SCPP C. DOPA/Sr.SCPP/ Silk fibroin	H&E H&E IHC	NBF Max in C VEGE and bFGF Max in C	(43)
Xie (2013)	SCPP	Gravity sintering	-	New Zealand white rabbits	15 x 5 mm defect above thighbone	12 W	A. HA B. CPP C. SCPP	H&E IHC x-ray microradiogr aphy	NBF: C>B>A VEGF: C>B>A	(44)
Gu (2013)	SCPP		Rabbit BMSCs	New Zealand white rabbits	15 mm segmental radius defect	4,8,16 W	A. HA B. CPP C. SCPP D.HA + MSCs E.CPP + MSCs F.SCPP + MSCs	H&E MT Toluidine blue x-ray microradiogr aphy	NBF 4th week D<E or F C,D,E,F significantly higher than A NBF 16th week F>E>C>B>D>A NBF in x-ray Max in F	(45)
Yang (2011)	HA + 10% Sr	Hydrothermal method	-	Female SD rat	5mm critical size calvarial defects	4, 12 W	A. COL B. COL + HA C. COL + HA + Sr	H&E MT CT	HU 1st month: A: 15.7 ± 3.3 B: 121 ± 14.2 C: 219.4 ± 37.1 HU 3rd month: A: 59.4 ± 8.5 B: 249.2 ± 20.5 C: 381.7 ± 25.3 NBF: B: 0.93 ± 0.07 C: 1.48 ± 0.13 Mature bone area (fold increase compared to A): B: 11.6 ± 0.6 C: 3.4 ± 0.7 β-catenin, OPN, COL1 C>B	(46)
Li (2010)	HA + Col + Sr	Sol-Gel	-	SD ovareictomized rat	1 mm intercondylar channel into medullary canal in tibiae	12 W	A.HA B.HA + Sr	μ-CT Toluidine blue	Bone area ratio: B= A + 70.9% Bone to implant contact: B=A + 49.9% BV/TV: A:24.7 ± 4.9 B: 42.9 ± 6.7 B=A + 73.7%	(47)

APMs: amorphous calcium phosphate porous microspheres; HVM: human Vimentin antibody; PBLG: poly(γ-benzyl-L-glutamate); PDIF: polydiisopropyl fumarate; rBMSC: rat bone marrow derived stem cells; SCPP: strontium doped calcium polyphosphate; Sr: Strontium; SRA: laponite-strontium ranelate.

Different parameters including X-ray radiography or computed tomography (CT) measured bone mineral density, micro-CT derived new bone volume, mechanical testings, Dual x-ray absorptiometry, histomorphomteric analysis with Haemotoxylin and Eosin (H&E) and Goldner-Masson's trichrome staining, quantitative real time polymerase chain reaction (qRT-PCR) measurement of different RNAs and western blot of the resultant proteins were evaluated. Other stainings such as von kossa for calcium detection, toluidine blue for cell nuclei, acid fuschin, fast green, sirius red for collagen, tartrate-resistant acid
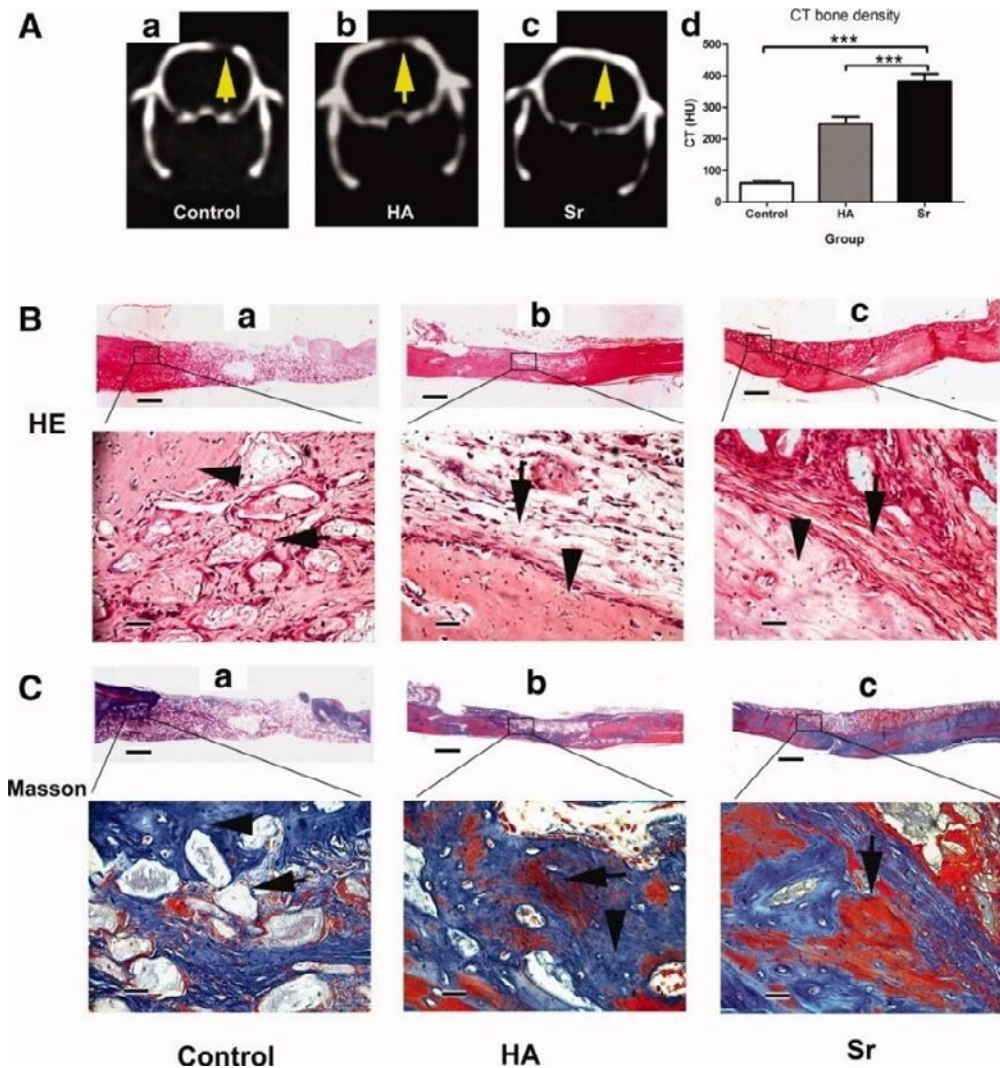
Figure 2. CT scanning and histological analysis of bone formation at 3 months after the transplantation. (A): Representative radiographic analysis of bone formation in the control (a), hydroxyapatite (HA) (b), and strontium (Sr) groups (c). (B): Representative histological analysis (H&E staining) of bone formation in the control (a), HA (b), and Sr group (c). (C): Representative histological analysis (Masson staining) of bone formation in the control (a), HA (b), and Sr group (c). Scale bar = 800 μm (B, C, low magnification); = 75 μm (B, C, high magnification). ***, p < .001. Abbreviations: CT, computed tomography; HA, hydroxyapatite; HU, Hounsfield unit; Sr, strontium (46). - The images are provided with permission from Stem Cells Publications, John Wiley & Sons Publication group (license number: 4755280758795).

phosphatase for osteoclast and giemsa for osteoblast as well as chloroacetate esterase for neutrophils and human vimentin antibody staining for endothelium was conducted in some studies. Immunohistochemistry analysis helped in identification of various osteogenic markers such as osteonectin, osteopontin, collagen type I, β-catenin as well as angiogenic factors such as vascular endothelial growth factors (VEGF), basic fibroblast growth factor (BFGF).

Discussion

Biomimetic bone scaffolds incorporating additional therapeutic agents like MITAs are a main focus of BTE. The specific biological advantage that these ions bring to scaffolds as well as other potential mechanical, and antimicrobial enhancements may vary depending on the ion entity, fabrication method, and biomaterials used. Herein, we categorized in-vivo studies on MITAs in bone substitutes with the aim of clarifying their efficacy and identifying the affecting parameters.

The most frequently used ion, strontium (Sr), is a naturally occurring ion with 98% of it localized in the skeleton, exchanged with Ca^{2+} in the HA crystal lattice (3). Sr^{2+}, a structurally similar ion to calcium, helps promote osteogenic differentiation of mesenchymal stem cells (MSCs) via wnt/βcatenin and Ras/MAPK signaling pathways (46) and inhibits osteoclastic activity. Strontium has thus been widely investigated in both *In-vitro* and *In-vivo* studies and has been shown to enhance NBF, remodeling and ossseointegration when added alone to scaffolds or combined with other ions (41, 66-68). However, high doses of Sr have been shown to have adverse effect on calcium absorption and bone mineralization, therefore, engineering a controlled release scaffold is of great importance (69). In our review, Sr enhanced NBF in nine studies while two studies had no control scaffolds without Sr to make the comparison possible. One study failed to report any significant difference between laponite-strontium ranelate containing PCL and PCL alone with or without cells (37) which could be due to ectopic implantation. Gao et al., reported bone volume/total volume (BV/TV) resembling that of natural bone using Sr-HA-graft-poly(benzyl-L-glutamate) nanocomposite microcarriers loaded with ADSCs in a mice 2mm critical-sized femoral defect model (42).

Magnesium was also extensively studied in combination with PLGA and PCL polymers and HA. Mg^{2+} is another element found in human body, half of which is deposited in bone tissue (70). Studies have shown a correlation between magnesium deficiency and osteoporosis, attributable to changes in parathyroid hormone (PTH), Vitamin D levels and increased pro-inflammatory cytokine secretion such as substance P, TNF-α, IL-1β, and RANKL (71). Similar to strontium, magnesium works by stimulating MSCs proliferation, differentiation while suppressing osteoclast activity. Moreover, it has been demonstrated that magnesium increases osteogenic gene expression and protein expression of collagen type X and VEGF (72). Additionally, magnesium is reported to have antibacterial properties, beneficial in reducing infection risk in bone grafting procedures (73). Almost all studies reviewed in this article, proved magnesium efficient in promoting NBF with the exception of a study by Suryavanshi et al. that reported no NBF using PCL and MgO in subcutaneous implantation. The scaffold, however, was proved to be biocompatible (48). In another study by Deng et al. in a goat bi-parietal 15 mm calvarial defect model, the synergistic effect of magnesium and human recombinant bone morphogenetic protein 2 (rh-BMP2) was also demonstrated (49).

Another frequently studied ion is zinc, a trace element essential for neural growth, immunological functions and many other cellular processes (74). Zinc is well recognized as a critical mineral for bone health and development, as its deficiency is associated with bone growth lag and mal-development as well as osteoporosis (75). Zn^{2+} affects MSCs through ERK1/2 signaling and hinders osteoclasts by antagonizing NF-κB pathway (76). Zinc also processes antibacterial effects owing to production of reactive oxygen species (ROS) and aids in wound healing (77). Of the five *In-vivo* studies reported in this study, one study provided no control for

comparison (53), while another study showed that both βTCP and Zn-TCP were able to stimulate regeneration of new bone closing the defect but Zn-TCP showed a faster rise in bone mineral density and resulted in a more mature and denser trabecular bone (54). A long-term (60 weeks) study on bone formation in white New Zealand rabbit transcortical femoral defect model also presented that Zn-HA-TCP was able to promote NBF compared to HA-TCP (55). Similar results were obtained in an 8-week study on Zn-HA-Collagen in SD rat model (52). Samanta et al. conducted a study in a rabbit femoral defect model where TCP-Zn was compared to TCP-Ti and TCP-Mg. NBF was increased to 65.06 ± 3.0 in TCP-Ti, compared to 50.55 ± 2.0 in TCP-Mg, 48.40 ± 2.0 in TCP-Zn, and 34.24 ± 2.0 in TCP alone (22). More similar studies are recommended to make the comparison between various ions possible.

Data on other less commonly applied metallic ions can be found in Table 1. The readers are referred to two published narrative reviews on metallic ions for further explanation of the functions of these ions (3, 72). Undoubtedly, the most frequently used ion in bone structure and bone substitutes is calcium. However, as their obvious role in bone tissue regeneration has been well documented, the authors agreed to limit this systematic review on ions, whose potential role and efficacy are yet to be determined. The authors also excluded studies on mixtures of ions and alloys as such studies would not help in drawing conclusions regarding the efficacy of a specific ion. There is a body of *In-vivo* literature on magnetic scaffolds, of which only the ones that housed animals in normal cages are included. Studies stimulating bone formation by creating a magnetic field around the animal during implantation period were excluded because it was agreed that the underlying mechanism is rather different than that of MITAs. The readers are kindly encouraged to read a review by Xu et al. on magnetic responsive scaffolds in BTE (78).

As presented in table 1, various polymers, ceramics and composites are functionalized using MITAs. Among the polymers, PCL seems to be more frequently used which could be explained by its relative simple application in the fabrication of scaffolds. PCL is a non-immunogenic synthetic polymer which can be dissolved in most of organic solvents, there are many methods to its fabrication and it can be blended with other polymers or ceramics to hand in composite scaffolds with enhanced mechanical properties especially in load bearing areas. The slow degradation rate and unfavorable water contact angle are among its drawbacks (79). Hydroxyapatite is the most applied ceramic doped with MITAs in our review. HA is a calcium phosphate similar to that of human hard tissues in morphology and composition with an identical Ca/P ratio to bone apatite. HA has been extensively used in BTE due to its stability in physiological conditions, biocompatibility, osteoinductivity and non-toxicity and non-inflammatory nature (80). In our review, HA was introduced into animal defects alone or with natural or synthetic polymers such as collagen, PLLA, PLGA and chitosan. Such composite scaffolds have the advantage of making the scaffold osteoconductive and reinforcing the mechanical characteristics of scaffold further mimicking natural bone architecture (81). The efficacy of MITAs in improving bone tissue regeneration was evaluated in mesoporous bioactive glasses (MBG) by some researchers. We excluded all these studies because as explained before, the specific influence of an ion could be obscured by the synergistic effect they may have with other ions in MBG. There is a valuable review on MBG incorporating MITAs for bone tissue engineering which can be considered in addition to the present study (82).

A meta-analysis by shanbhag et al. indicated statistically significant benefits in loading scaffolds with cells with a weighted mean difference of NBF of 15.59–49.15% and 8.60–13.85% NBF in large- and small-animal models, respectively (83). In our review, seven studies seeded the scaffolds with various types of cells. In one study, hypoxia preconditioned BMSCs enhanced NBF more than normal BMSCs and they both scored higher NBF compared to unloaded HA + Li scaffold (8). Wang et al. and Gu et al. loaded all scaffolds with cells and prabha et al. reported no enhancement of NBF when loading scaffolds with hBMSCs (10, 37, 84). Yan et al. and Gao

et al. also showed improved NBF using rabbit and mouse ADSCs (40, 42).

Animal models play a crucial role in testing bone scaffolds for understanding their osteoconductivity, biocompatibility, mechanical properties, degradation, and interaction with host tissues (85). Small animal models used in BTE research are primarily rodents (rats and mice) and rabbits (83). In our review, almost all studies used small animals because of significantly lower costs, and easier housing and handling (86). Rodents also have a less varied genetic background in terms of biological response which makes the statistical analysis credible (87). However, before generalizing results from these studies to humans, the differences in the structure and composition of these animals' bones as well as faster skeletal change and bone turnover in these animals should be considered (88). Another limitation is the inability to create multiple defects to study different materials simultaneously (89). In two studies, larger animals, namely beagle dogs and goats were used. Dogs are widely used in musculoskeletal research, given the similarities in structure and physiology of canine and human bone. However, limitations of ethical issues, high costs, handling difficulties exist (89). One study used normal human osteoblast cell line, claiming that it mimics the cellular event of the *in-vivo* intramembranous bone formation process and reported the study as an *In-vivo* model which was excluded by the agreement of authors (90).

Critical-sized defects were created in these animal models in order to observe osteoinductive capacity of scaffolds incorporating MITAs. A critical-sized defect is defined as "the smallest osseous wound that does not heal spontaneously over a long period of time or more clinically relevant, that which has no mineralized area > 30% after 52 weeks" (85). For the rat calvarial defect, 8 mm is generally reported to be the critical size; however, smaller defects have been investigated in models with bi-parietal defects, resulting in fewer sacrificed animals (91). In our review, nine articles regarded 5 mm defects as critical which is suggested to be replaced with 8 mmm defects in future studies. Three studies evaluated the newly designed

scaffolds in subcutaneous implantation, two of which could not report NBF (10, 37, 48). Therefore, it is suggested that more accurate defect models be used in BTE researches.

The most frequently conducted test to evaluate I*n-vivo* bone formation were μ-CT, and H&E staining. The biological performances of a scaffold regarding cell adhesion, proliferation and mineral deposition as well as formation of mature bone with vasculature are factors to be evaluated during *In-vivo* implantation testing (92). μ-CT is a non-destructive computational technique capable of providing 3D images of engineered constructs as well as quantitative data based on the fact that new bone, fibrous tissue and scaffolds have different coefficients of absorption (93). Studies have also focused on other aspects of bone substitutes containing MITAs such as in tumor suppression capability, angiogenetic ability, immune response induction, etc. (94-96). However, all the articles not evaluating the formation of new bone were excluded in our study because they were not consistent with the aims of this review.

Limitations

Few studies did not have the control group, and several variations including cell sources, scaffold types, fabrication methods, and measured parameters between included studies do not permit general conclusions to be drawn.

Conclusion

A systematic review on *In-vivo* studies on MITAs used in Bone tissue engineering showed several important findings: 1) various materials can be successfully used to incorporate MITAs and one must opt for the composition that renders the best biological response as well as physicochemical characteristics. 2) Of the various fabrication methods applied in BTE for integrating MITAs into scaffolds, it is important to consider their effect on controlled release of ion besides the ease of method as many ions can have deleterious effects if the therapeutic doses are surpassed. 3) A tendency to enhance new bone formation with the use of MITAs can be observed in the studies. However, this needs

to be validated with further studies comparing various ions with each other and the different concentration in the same animal model using critical-sized defects.

report.

References

1. Scheller EL, Krebsbach PH and Kohn DH. Tissue engineering: state of the art in oral rehabilitation. *J. Oral Rehabil.* (2009) 36: 368-89.

2. Motamedian SR, Hosseinpour S, Ahsaie MG and Khojasteh A. Smart scaffolds in bone tissue engineering: A systematic review of literature. *World J. Stem Cells* (2015) 7: 657.

3. Mourino V, Cattalini JP and Boccaccini AR. Metallic ions as therapeutic agents in tissue engineering scaffolds: an overview of their biological applications and strategies for new developments. *J. R. Soc. Interface* (2012) 9: 401-19.

4. Bostancioglu RB, Gurbuz M, Akyurekli AG, Dogan A, Koparal AS and Koparal AT. Adhesion profile and differentiation capacity of human adipose tissue derived mesenchymal stem cells grown on metal ion (Zn, Ag and Cu) doped hydroxyapatite nano-coated surfaces. *Colloids Surf. B Biointerfaces* (2017) 155: 415-28.

5. Sánchez AHM, Omidi M, Wurlitzer M, Fuh MM, Feyerabend F, Schlüter H, Willumeit-Römer R and Luthringer B. Proteome analysis of human mesenchymal stem cells undergoing chondrogenesis when exposed to the products of various magnesium-based materials degradation. *Bioactive Materials* (2019) 4: 168-88.

6. Prashanth L, Kattapagari K, Chitturi R, Baddam V and Prasad L. A review on role of essential trace elements in health and disease. *J. NTR Univ. Health Sci.* (2015) 4: 75-85.

7. Qiao W, Liu R, Li Z, Luo X, Huang B, Liu Q, Chen Z, Tsoi J, Su Y, Cheung, Matinlinna J, Yeung K and Chen Z. Contribution of the in situ release of endogenous cations from xenograft bone driven by fluoride incorporation toward enhanced bone regeneration. *Biomater Sci.* (2018) 6: 2951-64.

8. Li D, Huifang L, Zhao J, Yang Z, Xie X, Wei Z, Li D and Kang P. Porous lithium-doped hydroxyapatite scaffold seeded with hypoxia-preconditioned bone-marrow mesenchymal stem cells for bone-tissue regeneration. *Biomed. Mater.* (2018) 13: 055002.

9. Yuan Z, Wei P, Huang Y, Zhang W, Chen F, Zhang X, Mao J, Chen D, Cai Q and Yang X. Injectable PLGA microspheres with tunable magnesium ion release for promoting bone regeneration. *Acta Biomater.* (2019) 85: 294-309.

10. Wang Y, Cui W, Chou J, Wen S, Sun Y and Zhang H. Electrospun nanosilicates-based organic/inorganic nanofibers for potential bone tissue engineering. *Colloids Surf. B Biointerfaces* (2018) 172: 90-7.

11. Zhang Q, Chen X, Geng S, Wei L, Miron RJ, Zhao Y and Zhang Y. Nanogel-based scaffolds fabricated for bone regeneration with mesoporous bioactive glass and strontium: *In-vitro* and *In-vivo* characterization. *J. Biomed. Mater. Res. A* (2017) 105: 1175-83.

12. Yu W, Sun TW, Qi C, Ding Z, Zhao H, Chen F, Chen D, Zhu Y, Shi Z and He Y. Strontium-Doped Amorphous Calcium Phosphate Porous Microspheres Synthesized through a Microwave-Hydrothermal Method Using Fructose 1,6-Bisphosphate as an Organic Phosphorus Source: Application in Drug Delivery and Enhanced Bone Regeneration. *ACS Appl. Mater. Interfaces* (2017) 9: 3306-17.

13. Liu YJ, Su WT and Chen PH. Magnesium and zinc borate enhance osteoblastic differentiation of stem cells from human exfoliated deciduous teeth *In-vitro*. *J Biomater. Appl.* (2018) 32: 765-74.

14. Drynda A, Drynda S, Kekow J, Lohmann CH and Bertrand J. Differential Effect of Cobalt and Chromium Ions as Well as CoCr Particles on the Expression of Osteogenic Markers and Osteoblast Function. *Int. J. Mol. Sci.* (2018) 19: 3034

15. Wang H, Zhao S, Zhou J, Shen Y, Huang W, Zhang C, Rahaman M and Wang D. Evaluation of borate bioactive glass scaffolds as a controlled delivery system for copper ions in stimulating osteogenesis and angiogenesis in bone healing. *J. Mater. Chem. B* (2014) 2: 8547-57.

16. Saini RK, Bagri LP and Bajpai A. Nano-silver hydroxyapatite based antibacterial 3D scaffolds of gelatin/alginate/poly (vinyl alcohol) for bone tissue engineering applications. *Colloids Surf. B Biointerfaces.* (2019) 177: 211-8.

17. Goudouri OM, Kontonasaki E, Lohbauer U and Boccaccini AR. Antibacterial properties of metal and metalloid ions in chronic periodontitis and peri-implantitis therapy. *Acta Biomater.* (2014) 10: 3795-810.

18. Park JS, Suryaprakash S, Lao Y-H and Leong KW. Engineering mesenchymal stem cells for regenerative medicine and drug delivery. *Methods* (2015) 84: 3-16.

19. Roseti L, Parisi V, Petretta M, Cavallo C, Desando G, Bartolotti I and Grigolo B. Scaffolds for Bone Tissue Engineering: State of the art and new perspectives. *Mat. Sci. Eng. C-Mater.* (2017) 78: 1246-62.

20. Hu C, Ashok D, Nisbet DR and Gautam V. Bioinspired surface modification of orthopedic implants for bone tissue engineering. *Biomaterials* (2019) 219: 119366.

21. Tripathi A, Saravanan S, Pattnaik S, Moorthi A, Partridge NC and Selvamurugan N. Bio-composite scaffolds containing chitosan/nano-hydroxyapatite/nano-copper–zinc for bone tissue engineering. *Int. J. Biol. Macromol.* (2012) 50: 294-9.

22. Samanta SK, Devi KB, Das P, Mukherjee P, Chanda A, Roy M and Nandi S. Metallic ion doped tri-calcium phosphate ceramics: Effect of dynamic loading on in vivo bone regeneration. *J. Mech. Behav. Biomed. Mater.* (2019) 96: 227-35.

23. O'Neill E, Awale G, Daneshmandi L, Umerah O and Lo KWH. The roles of ions on bone regeneration. *Drug Discov. Today* (2018) 23: 879-90.

24. Sansone V, Pagani D and Melato M. The effects on bone cells of metal ions released from orthopaedic implants. A review. *Clin. Cases Miner. Bone Metab.* (2013) 10: 34-40.

25. De Jong WH, De Rijk E, Bonetto A, Wohlleben W, Stone V, Brunelli A, Badetti E, Marcomini A, Gosens I and Cassee F. Toxicity of copper oxide and basic copper carbonate nanoparticles after short-term oral exposure in rats. *Nanotoxicology* (2019) 13: 50-72.

26. Apaza-Bedoya K, Bijukumar D, Benfatti CAM, Mathew MT, da Silva JSP and Souza JCM. Chapter 4 - Adverse local and systemic effect of nanoparticles released from oral and cranio-maxillofacial implants. In: Souza JCM, Hotza D, Henriques B, Boccaccini AR. (eds). Nanostructured Biomaterials for Cranio-Maxillofacial and Oral Applications: Elsevier (2018) 63-79.

27. Wu C, Zhou Y, Fan W, Han P, Chang J, Yuen J, Zhang M and Xiao Y. Hypoxia-mimicking mesoporous bioactive glass scaffolds with controllable cobalt ion release for bone tissue engineering. *Biomaterials* (2012) 33: 2076-85.

28. Fielding G and Bose S. SiO2 and ZnO dopants in three-dimensionally printed tricalcium phosphate bone tissue engineering scaffolds enhance osteogenesis and angiogenesis *In-vivo*. *Acta Biomater.* (2013) 9: 9137-48.

29. Forero JC, Roa E, Reyes JG, Acevedo C and Osses N. Development of Useful Biomaterial for Bone Tissue Engineering by Incorporating Nano-Copper-Zinc Alloy (nCuZn) in Chitosan/Gelatin/Nano-Hydroxyapatite (Ch/G/nHAp) Scaffold. *Materials (Basel).* (2017) 10: 1177

30. Brown A, Zaky S, Ray H, Jr. and Sfeir C. Porous magnesium/PLGA composite scaffolds for enhanced bone regeneration following tooth extraction. *Acta Biomater.* (2015) 11: 543-53.

31. Fernandes JS, Gentile P, Martins M, Neves NM, Miller C, Crawford A, Pires R, Hatton P and Reis R. Reinforcement of poly-l-lactic acid electrospun membranes with strontium borosilicate bioactive glasses for bone tissue engineering. *Acta Biomater.* (2016) 44: 168-77.

32. Newby PJ, El-Gendy R, Kirkham J, Yang XB, Thompson ID and Boccaccini AR. Ag-doped 45S5 Bioglass(R)-based bone scaffolds by molten salt ion exchange: processing and characterisation. *J. Mater. Sci. Mater. Med.* (2011) 22: 557-69.

33. Tsai KY, Lin HY, Chen YW, Lin CY, Hsu TT and Kao CT. Laser Sintered Magnesium-Calcium Silicate/Poly-epsilon-Caprolactone Scaffold for Bone Tissue Engineering. *Materials (Basel).* (2017) 10: 65.

34. Mouriño V, Vidotto R, Cattalini J and Boccaccini A. Enhancing biological activity of bioactive glass scaffolds by inorganic ion delivery for bone tissue engineering. *Curr. Opin. Biomed. Eng.* (2019).

35. Moher D, Liberati A, Tetzlaff J and Altman DG. Preferred Reporting Items for Systematic Reviews and Meta-Analyses: The PRISMA Statement. *J. Clin. Epidemiol.* (2009) 62: 1006-12.

36. Liu D, Nie W, Li D, Wang W, Zheng L, Zhang J, Zhang J, Peng Ch, Mo X and He Ch. 3D printed PCL/SrHA scaffold for enhanced bone regeneration. *Chem. Eng.* (2019) 362: 269-79.

37. Prabha RD, Nair BP, Ditzel N, Kjems J, Nair PD and Kassem M. Strontium functionalized scaffold for bone tissue engineering. *Mat. Sci. Eng. C-Mater.* (2019) 94: 509-15.

38. Lino AB, McCarthy AD and Fernandez JM. Evaluation of Strontium-Containing PCL-PDIPF Scaffolds for Bone Tissue Engineering: *In-vitro* and *In-vivo* Studies. *Ann. Biomed. Eng.* (2019) 47: 902-12.

39. Han X, Zhou X, Qiu K, Feng W, Mo H, Wang M, Wang J and He C. Strontium-incorporated mineralized PLLA nanofibrous membranes for promoting bone defect repair. *Colloids surf. B. Biomaterials* (2019) 179: 363-73.

40. Yan S, Xia P, Xu S, Zhang K, Li G, Cui L and Yin J. Nanocomposite Porous Microcarriers Based on Strontium-Substituted HA- g-Poly(gamma-benzyl-l-glutamate) for Bone Tissue Engineering. *ACS Appl. Mater. Interfaces* (2018) 10: 16270-81.

41. Ge M, Ge K, Gao F, Yan W, Liu H, Xue L, Jin Y, Ma H and Zhang J. Biomimetic mineralized strontium-doped hydroxyapatite on porous poly(l-lactic acid) scaffolds for bone defect repair. *Int. J. Nanomedicine* (2018) 13: 1707-21.

42. Gao L, Huang Z, Yan S, Zhang K, Xu S, Li G, Cui L and Yin J. Sr-HA-graft-Poly(gamma-benzyl-l-glutamate) Nanocomposite Microcarriers: Controllable Sr(2+) Release for Accelerating Osteogenenisis and Bony Nonunion Repair. *Biomacromolecules* (2017) 18: 3742-52.

43. Wang X, Gu Z, Jiang B, Li L and Yu X. Surface modification of strontium-doped porous bioactive ceramic scaffolds via poly(DOPA) coating and immobilizing silk fibroin for excellent angiogenic and osteogenic properties. *Biomater. Sci.* (2016) 4: 678-88.

44. Xie H, Wang J, Li C, Gu Z, Chen Q and Li L. Application of strontium doped calcium polyphosphate bioceramic as scaffolds for bone tissue engineering. *Ceram. Int.* (2013) 39: 8945-54.

45. Gu Z, Zhang X, Li L, Wang Q, Yu X and Feng T. Acceleration of segmental bone regeneration in a rabbit model by strontium-doped calcium polyphosphate scaffold through stimulating VEGF and bFGF secretion from osteoblasts. *Mat. Sci. Eng. C-Mater.* (2013) 33: 274-81.

46. Yang F, Yang D, Tu J, Zheng Q, Cai L and Wang L. Strontium enhances osteogenic differentiation of mesenchymal stem cells and *In-vivo* bone formation by activating Wnt/catenin signaling. *Stem Cells.* (2011) 29: 981-91.

47. Li Y, Li Q, Zhu S, Luo E, Li J, Feng G, Liao Y and Hu J. The effect of strontium-substituted hydroxyapatite coating on implant fixation in ovariectomized rats. *Biomaterials* (2010) 31: 9006-14.

48. Suryavanshi A, Khanna K, Sindhu K, Bellare J and Srivastava R. Magnesium oxide nanoparticle-loaded polycaprolactone composite electrospun fiber scaffolds for bone–soft tissue engineering applications: *In-vitro* and *In-vivo* evaluation. *Biomed. Mater.* (2017) 12: 055011.

49. Deng L, Li D, Yang Z, Xie X and Kang P. Repair of the calvarial defect in goat model using magnesium-doped porous hydroxyapatite combined with recombinant human bone morphogenetic protein-2. *Biomed. Mater. Eng.* (2017) 28: 361-77.

50. Laurenti M, Al Subaie A, Abdallah MN, Cortes AR, Ackerman JL, Vali H, Basu K, Zhang Y, Murshed M, Strandman S, Zhu J, Makhoul N, Barralet J and Tamimi F. Two-Dimensional Magnesium Phosphate Nanosheets Form Highly Thixotropic Gels That Up-Regulate Bone Formation. *Nano Lett.* (2016) 16: 4779-87.

51. Wong HM, Chu PK, Leung FKL, Cheung KMC, Luk KDK and Yeung KWK. Engineered polycaprolactone–magnesium hybrid biodegradable porous scaffold for bone tissue engineering. *Prog. Nat. Sci-Mater.* (2014) 24: 561-7.

52. Yu W, Sun TW, Qi C, Ding Z, Zhao H, Zhao S, Shi Z, Zhu Y, Chen D and He Y. Evaluation of zinc-doped mesoporous hydroxyapatite microspheres for the construction of a novel biomimetic scaffold optimized for bone augmentation. *Int. J. Nanomedicine* (2017) 12: 2293-306.

53. Begam H, Nandi SK, Chanda A and Kundu B. Effect of bone morphogenetic protein on Zn-HAp and Zn-HAp/collagen composite: A systematic *In-vivo* study. *Res Vet Sci.* (2017) 115: 1-9.

54. Chou J, Hao J, Kuroda S, Bishop D, Ben-Nissan B, Milthorpe B and Otsuka M. Bone regeneration of rat tibial defect by zinc-tricalcium phosphate (Zn-TCP) synthesized from porous Foraminifera carbonate macrospheres. *Mar. Drugs* (2013) 11: 5148-58.

55. Kawamura H, Ito A, Muramatsu T, Miyakawa S, Ochiai N and Tateishi T. Long-term implantation of zinc-releasing calcium phosphate ceramics in rabbit femora. *J. Biomed. Mater. Res. B Appl. Biomater.* (2003) 65: 468-74.

56. Cui W, Sun G, Qu Y, Xiong Y, Sun T, Ji Y, Yang L, Shao Z, Ma J, Zhang S and Guo X. Repair of rat calvarial defects using Si-doped hydroxyapatite scaffolds loaded with a bone morphogenetic protein-2-related peptide. *J. Orthop. Res.* (2016) 34: 1874-82.

57. Ma Y, Li Y, Hao J, Ma B, Di T and Dong H. Evaluation of the degradation, biocompatibility and osteogenesis behavior of lithium-doped calcium polyphosphate for bone tissue engineering. *Biomed. Mater. Eng.* (2019) 30: 23-36.

58. Russo A, Bianchi M, Sartori M, Boi M, Giavaresi G, Salter DM, Jelic M, Maltarello M, Ortolani A, Sprio S, Fini M, Tampieri A and Marcacci M. Bone regeneration in a rabbit critical femoral defect by means of magnetic hydroxyapatite macroporous scaffolds. *J. Biomed. Mater. Res. B.* (2018) 106: 546-54.

59. De Santis R, Russo A, Gloria A, D'Amora U, Russo T, Panseri S, Sandri M, Tampieri A, Marcacci M, Dediu V, Wilde C and Ambrosio L. Towards the Design of 3D Fiber-Deposited Poly(-caprolactone)/Iron-Doped Hydroxyapatite Nanocomposite Magnetic Scaffolds for Bone Regeneration. *J. Biomed. Nanotechnol.* (2015) 11: 1236-46.

60. D'Mello S, Elangovan S, Hong L, Ross RD, Sumner DR and Salem AK. Incorporation of copper into chitosan scaffolds promotes bone regeneration in rat calvarial defects. *J. Biomed. Mater. Res. B (* 2015) 103: 1044-9.

61. Wei P, Yuan Z, Cai Q, Mao J and Yang X. Bioresorbable Microspheres with Surface-Loaded Nanosilver and Apatite as Dual-Functional

Injectable Cell Carriers for Bone Regeneration. *Macromol. Rapid Comm.* (2018) 39: e1800062.

62. Perez RA, Kim JH, Buitrago JO, Wall IB and Kim HW. Novel therapeutic core-shell hydrogel scaffolds with sequential delivery of cobalt and bone morphogenetic protein-2 for synergistic bone regeneration. *Acta Biomater.* (2015) 23: 295-308.

63. Gao C, Li C, Wang C, Qin Y, Wang Z, Yang F, Liu H, Chang F and Wang J. Advances in the induction of osteogenesis by zinc surface modification based on titanium alloy substrates for medical implants. *J. Alloy Compd.* (2017) 726: 1072-84.

64. Deng L, Deng Y and Xie K. AgNPs-decorated 3D printed PEEK implant for infection control and bone repair. *Colloids surf. B Biomaterials.* (2017) 160: 483-92.

65. Chou J, Hao J, Hatoyama H, Ben-Nissan B, Milthorpe B and Otsuka M. Effect of biomimetic zinc-containing tricalcium phosphate (Zn-TCP) on the growth and osteogenic differentiation of mesenchymal stem cells. *J. Tissue Eng. Regen.* (2015) 9: 852-8.

66. Kargozar S, Lotfibakhshaiesh N, Ai J, Mozafari M, Brouki Milan P, Hamzehlou S, Barati M, Baino F, Hill R, and Joghataei M. Strontium- and cobalt-substituted bioactive glasses seeded with human umbilical cord perivascular cells to promote bone regeneration via enhanced osteogenic and angiogenic activities. *Acta Biomater.* (2017) 58: 502-14.

67. Goodarzi H, Hashemi-Najafabadi S, Baheiraei N and Bagheri F. Preparation and Characterization of Nanocomposite Scaffolds (Collagen/beta-TCP/SrO) for Bone Tissue Engineering. *J. Tissue Eng. Regen.* (2019) 16: 237-51.

68. Mao L, Xia L, Chang J, Liu J, Jiang L, Wu C and Fang B. The synergistic effects of Sr and Si bioactive ions on osteogenesis, osteoclastogenesis and angiogenesis for osteoporotic bone regeneration. *Acta Biomater.* (2017) 61: 217-32.

69. Grynpas MD, Hamilton E, Cheung R, Tsouderos Y, Deloffre P, Hott M and Marie P. Strontium increases vertebral bone volume in rats at a low dose that does not induce detectable mineralization defect. *Bone* (1996) 18: 253-9.

70. Walker J, Shadanbaz S, Woodfield TB, Staiger MP and Dias GJ. Magnesium biomaterials for orthopedic application: a review from a biological perspective. *J. Biomed. Mater. Res. B.* (2014) 102: 1316-31.

71. Castiglioni S, Cazzaniga A, Albisetti W and Maier JAM. Magnesium and osteoporosis: current state of knowledge and future research directions. *Nutrients* (2013) 5: 3022-33.

72. O'Neill E, Awale G, Daneshmandi L, Umerah O and Lo KW. The roles of ions on bone regeneration. *Drug Discov. Today* (2018) 23: 879-90.

73. Ma R, Lai Y-x, Li L, Tan H-l, Wang J-l, Li Y, Tang T and Qin L. Bacterial inhibition potential of 3D rapid-prototyped magnesium-based porous composite scaffolds–an *In-vitro* efficacy study. *Sci. Rep.* (2015) 5: 13775.

74. Chasapis CT, Loutsidou AC, Spiliopoulou CA and Stefanidou ME. Zinc and human health: an update. *Arch. Toxicol.* (2012) 86: 521-34.

75. Kwun IS, Cho YE, Lomeda RA, Shin HI, Choi JY, Kang YH and Beattie J. Zinc deficiency suppresses matrix mineralization and retards osteogenesis transiently with catch-up possibly through Runx 2 modulation. *Bone* (2010) 46: 732-41.

76. Yamaguchi M and Weitzmann MN. Zinc stimulates osteoblastogenesis and suppresses osteoclastogenesis by antagonizing NF-kappaB activation. *Mol. Cell Biochem.* (2011) 355: 179-86.

77. Xu Q, Zheng Z, Wang B, Mao H and Yan F. Zinc ion coordinated poly (ionic liquid) antimicrobial membranes for wound healing. *ACS Appl. Mater. Interfaces* (2017) 9: 14656-64.

78. Xu H-Y and Gu N. Magnetic responsive scaffolds and magnetic fields in bone repair and regeneration. *Front. Mater. Sci.* (2014) 8: 20-31.

79. Abedalwafa M, Wang F, Wang L and Li C. Biodegradable poly-epsilon-caprolactone (PCL) for tissue engineering applications: a review. *Rev. Adv. Mater. Sci.* (2013) 34: 123-40.

80. Wei G and Ma PX. Structure and properties of nano-hydroxyapatite/polymer composite scaffolds for bone tissue engineering. *Biomaterials* (2004) 25: 4749-57.

81. Wang M. Composite scaffolds for bone tissue engineering. *Am. J. Biochem. Biotechnol.* (2006) 2: 80-4.

82. Mouriño V, Vidotto R, Cattalini JP and Boccaccini AR. Enhancing biological activity of bioactive glass scaffolds by inorganic ion delivery for bone tissue engineering. *Curr. Opin. Biomed.* (2019) 10: 23-34.

83. Shanbhag S, Pandis N, Mustafa K, Nyengaard JR and Stavropoulos A. Alveolar bone tissue engineering in critical-size defects of experimental animal models: a systematic review and meta-analysis. *J. Tissue Eng. Regen.* (2017) 11: 2935-49.

84. Gu Z, Xie H, Li L, Zhang X, Liu F and Yu X. Application of strontium-doped calcium polyphosphate scaffold on angiogenesis for bone tissue engineering. *J. Mater. Sci.: Mater. Med.* (2013) 24: 1251-60.

85. Li Y, Chen S-K, Li L, Qin L, Wang X-L and Lai Y-X. Bone defect animal models for testing efficacy

of bone substitute biomaterials. *J. Orthop. Transl.* (2015) 3: 95-104.

86. Gomes PS and Fernandes MH. Rodent models in bone-related research: the relevance of calvarial defects in the assessment of bone regeneration strategies. *Lab Anim*. (2011) 45: 14-24.

87. Stavropoulos A, Sculean A, Bosshardt DD, Buser D and Klinge B. Pre-clinical *In-vivo* models for the screening of bone biomaterials for oral/craniofacial indications: focus on small-animal models. *Periodontol 2000*. (2015) 68: 55-65.

88. Castaneda S, Largo R, Calvo E, Rodriguez-Salvanes F, Marcos ME, Diaz-Curiel M and Herrero-Beaumont G. Bone mineral measurements of subchondral and trabecular bone in healthy and osteoporotic rabbits. *Skeletal Radiol*. (2006) 35: 34-41.

89. Pearce AI, Richards RG, Milz S, Schneider E and Pearce SG. Animal models for implant biomaterial research in bone: a review. *Eur. Cell Mater*. (2007) 13: 1-10.

90. John Ł, Podgórska M, Nedelec J-M, Cwynar-Zając Ł and Dzięgiel P. Strontium-doped organic-inorganic hybrids towards three-dimensional scaffolds for osteogenic cells. *Mat. Sci. Eng. C-Mater*. (2016) 68: 117-27.

91. Spicer PP, Kretlow JD, Young S, Jansen JA, Kasper FK and Mikos AG. Evaluation of bone regeneration using the rat critical size calvarial defect. *Nat*. (2012) 7: 1918-29.

92. Livingston T, Ducheyne P and Garino J. *In-vivo* evaluation of a bioactive scaffold for bone tissue engineering. *J. Biomed. Mater. Res. A*. (2002) 62: 1-13.

93. Barbetta A, Bedini R, Pecci R and Dentini M. Role of X-ray microtomography in tissue engineering. *Ann. Ist. Super Sanita*. (2012) 48: 10-8.

94. Oledzka E, Sobczak M, Kolmas J and Nalecz-Jawecki G. Selenium-substituted hydroxyapatite/biodegradable polymer/pamidronate combined scaffold for the therapy of bone tumour. *Int. J. Mol.* (2015) 16: 22205-22.

95. Liu Y, Li T, Ma H, Zhai D, Deng C, Wang J, Zhuo Sh, Chang J and Wu Ch. 3D-printed scaffolds with bioactive elements-induced photothermal effect for bone tumor therapy. *Acta Biomater*. (2018) 73: 531-46.

96. Diaz-Rodriguez P, Gomez-Amoza JL and Landin M. The synergistic effect of VEGF and bimorphic silicon carbides topography on *In-vivo* angiogenesis and human bone marrow derived mesenchymal stem cell differentiation. *Biomed. Mater*. (2015) 10: 045017.

This article is available online at http://www.ijpr.ir